EAI Endorsed Transactions
on Energy Web
Research Article **EAI.EU**

An Integrated MOPSO and Fuzzy Decision-Making Algorithmic Framework for Multi-Objective Configuration in High-Proportion Renewable Networks

Yuanping Guo[1,*], Yilin Zhong[1], Xingyan Liu[1], Ja Yin[1], Jie Wang[1]

[1]Power Grid Planning and Research Center, Guizhou Power Grid Co., Ltd., Guiyang 550000, China

Abstract

The optimal sizing and configuration of energy storage in networks with high renewable penetration represent a highly complex, multi-constraint, and non-linear optimization problem. Existing planning methods often struggle with premature convergence and lack systematic multi-criteria evaluation for high-dimensional scenarios. This paper proposes a data-driven optimization and evaluation framework integrating a modified Multi-Objective Particle Swarm Optimization (MOPSO) algorithm and fuzzy mathematics based on deep learning. First, a time-series production simulation model is established to capture dynamic supply-demand interactions. The MOPSO algorithm is then introduced, utilizing a non-linear adaptive decreasing inertia weight and a Pareto dominance-based update strategy to effectively maintain population diversity and avoid local optima. Finally, to select the best compromise solution from the generated Pareto optimal solution set, a fuzzy membership evaluation algorithm is applied. Simulation on a 20 GW renewable base (16 GW wind + 4 GW PV) with 4 GW thermal regulation shows that a 6-hour storage yields generation costs of 0.3002–0.4061 CNY/kWh. The proposed MOPSO outperforms NSGA-II in convergence and solution quality, and fuzzy membership enables optimal trade-off selection.

Keywords: fuzzy decision-making; pareto optimality; data-driven optimization; deep learning; renewable networks

Received on 22 January 2026, accepted on 09 March 2026, published on 28 July 2026

doi: 10.4108/ew.14209

1. Introduction

Battery energy storage systems (BESSs) and transmission infrastructure play critical roles in mitigating the variability and uncertainty of renewable energy sources (RESs). Santos et al. [1] investigated the influence of BESSs on transmission grid operation, highlighting their ability to enhance grid flexibility. Conlon et al. [2] assessed the trade-offs between new transmission lines and energy storage. Similarly, Peker et al. [3] demonstrated the benefits of combining transmission switching with high renewable penetration. At the European scale, Golombek et al. [4] analyzed the roles of transmission expansion towards 2050, emphasizing their complementary nature.

Beyond these system-level studies, various technological and operational aspects have been explored. Liu et al. [5] reviewed the control techniques and demand response of virtual power plants integrating RESs and energy storage. Wu et al. [6] proposed a robust co-planning model for AC/DC transmission networks and energy storage under renewable uncertainty. The impact of distributed energy storage on power quality was examined by Adewumi et al. [7]. Vellingiri et al. [8] developed a hybrid optimization algorithm for estimating the maximum hosting capacity of renewables.

Li et al. [9] assessed the pumped storage to reduce renewable curtailment and CO_2 emissions. Urban power management with energy storage integration was addressed by Arun et al. [10-12]. A multi-criteria assessment of energy storage benefits was presented by Malka et al. [13].

Mobile energy storage has also gained attention [14-20]. Li et al. [21] conducted an economic analysis of large-scale renewable energy storage technologies. Finally, Shafiei et

*Corresponding author. Email: guoyuanping1990@163.com

al. [22] proposed a planning framework for network systems with renewable resources and BESSs, focusing on resilience enhancement.

Despite the extensive research on energy storage and transmission planning, most existing studies focus on either bulk transmission systems with AC interconnections or distribution networks. In such a scenario, the coordination between local load demand and external transmission power requirements introduces unique challenges. The need to maintain reliable DC transmission while minimizing operational costs and renewable curtailment calls for dedicated optimal configuration and evaluation methods [23]. To further improve renewable energy accommodation, integrated operation strategies involving mobile energy storage systems, power networks, and transportation systems have been proposed to enhance renewable penetration rates [24]. Meanwhile, large-scale energy storage technologies, such as pumped hydro storage, have been extensively evaluated for their capability to reduce renewable curtailment and carbon emissions in renewable-dominated power systems [25].

This paper proposes a novel evaluation method for power source and energy storage planning in high-proportion renewable energy DC transmission scenarios. Simulation verification is conducted using a planning year scenario of a renewable energy base in northern China. The proposed method can effectively reduce system operating costs while meeting local demand and external transmission requirements, thereby improving the transmission efficiency of the DC transmission channel.

2. Optimal Configuration Model of Energy Storage in a New Energy Base

This paper takes a new energy base integrating new energy power generation, active regulating power sources, and an energy storage system as the research object. The power collection, step-up, and transmission losses of various power sources are ignored, and the equipment technical constraints, as well as network voltage constraints, are not considered for the time being. The local load refers to the portion of the regional load borne by the new energy base, which is primarily supplied by the new energy and energy storage within the base. The power from the active regulating power sources is transmitted outwards in coordination with the internal new energy and is not supplied to the local load.

2.1. New Energy Base Model

2.1.1. New Energy Power Generation Model

First, the new energy power output coefficient $\omega_{k,t}^{R}$ (the output coefficient of the new energy station k at time t) is introduced. Power curtailment is allowed during the operation simulation process; that is, when the system's regulating power sources are limited, it is permissible to curtail the active power of new energy.

$$P_{k,t}^{R} + P_{k,t}^{R,Cur} = \omega_{k,t}^{R} C_{k}^{R}, \quad \forall k,t \tag{1}$$

$$P_{k,t}^{R}, P_{k,t}^{R,Cur} \geq 0, \quad \forall k,t \tag{2}$$

where $P_{k,t}^{R}$ and $P_{k,t}^{R,Cur}$ are the generated power and curtailed power of the new energy station/plant k at time t, respectively; C_{k}^{R} is the rated installed capacity of the new energy station/plant k.

2.1.2. Active Regulating Power Source Model

New energy bases in China are mainly located in the Northeast and Northwest regions, where the active regulating power sources within the bases are predominantly thermal power units. In this paper, they are simplified as power sources with a specific power regulation range, and the differences in active power output constraints among various types of units are neglected.

$$\alpha_{min} C_{i}^{I} \leq P_{i,t}^{I} \leq \alpha_{max} C_{i}^{I}, \quad \forall i,t \tag{3}$$

where I is the set of active regulating power sources; $P_{i,t}^{I}$ is the active power output of the active regulating power source at time t; C_{i}^{I} is the rated capacity of the active regulating power source; α_{min} and α_{max} are the lower and upper limit constraint coefficients for the active power output of the active regulating power source, respectively.

This paper focuses on power-source-side planning, and the generation operating cost model is adopted for the thermal power units serving as flexible power sources:

$$F^{I} = \sum_{t=1}^{N_T} \sum_{i=1}^{N_I} I_{g}^{P} P_{i,t}^{I} \tag{4}$$

where F^{I} is the annual operating cost of the regulating power sources (thermal power) in the new energy base; I_{g}^{P} is the unit operating cost of the thermal power units.

2.1.3. Energy Storage Model

This paper focuses on the hourly-level power and energy balance, while ignoring the rapid, short-term frequency regulation requirements in primary and secondary frequency regulation scenarios. The operational constraints of energy storage are formulated as power output constraints.

$$\begin{cases} E_{b,t}^{B} - E_{b,t-1}^{B} = \eta_{b}^{B} P_{b,t}^{B,cha} - P_{b,t}^{B,dis} / \eta_{b}^{B}, & \forall b,t \\ E_{b,t=0}^{B} = E_{b,t=N_T}^{B} = \lambda_{b}^{B,min} H_{b} P_{b}^{B}, & \forall b,t \end{cases} \tag{5}$$

$$\begin{cases} 0 \leq P_{b,t}^{B,cha}, P_{b,t}^{B,dis} \leq P_{b}^{B}, & \forall b,t \\ 0 \leq E_{b,t}^{B} \leq H_{b} P_{b}^{B}, & \forall b,t \end{cases} \tag{6}$$

where P_{b}^{B} and H_{b} are the maximum charging/discharging power and the sustainable discharging duration of the energy storage system, respectively, which represent the two core parameters to be optimized in this paper; $P_{b,t}^{B,cha}$ and $P_{b,t}^{B,dis}$ are the charging power and discharging power of the energy storage system at the current moment, respectively; Equation (5) is the energy balance equation of the energy storage system; $E_{b,t}^{B}$ denotes the capacity of the energy storage system at time t; η_b^B is the charging and discharging efficiency of the energy storage system; N_T is the energy storage cycle; $\lambda_b^{B,min}$ is the power output constraint coefficient.

2.1.4. Power Outbound Delivery Model

The power outbound delivery model is based on the outbound delivery demand curve, and the primary constraints include the power balance constraint and the outbound electricity guarantee rate constraint.

$$P_{k,t}^{R} + P_{i,t}^{I} + P_{b,t}^{B,dis} - P_{b,t}^{B,cha} - P_{L,t} = F_t, \quad \forall k,b,t \tag{7}$$

$$F_t + L_t^{lack} = L_t, \quad \forall t \tag{8}$$

$$0 \le L_t^{lack} \le L_t, \quad \forall t \tag{9}$$

$$G^{elec} = \left(\frac{\sum_{t=1}^{T} L_t - \sum_{t=1}^{T} L_t^{lack}}{\sum_{t=1}^{T} L_t} \right) \times 100\% \tag{10}$$

where F_t is the actual outbound delivery power of the new energy base at time t; $P_{L,t}$ is the internal load demand power of the new energy base, which must be fully guaranteed; L_t and L_t^{lack} are the target outbound delivery power and power shortage at time t, respectively. Equation (7) represents the power balance equation, and Equation (10) defines the outbound electricity guarantee rate G^{elec} for the simulation cycle T.

2.2. Optimal Configuration Model of Energy Storage Considering Both Economy and Reliability

The objective is to minimize the targeted economic cost, which includes two components: investment cost and operating cost.

The investment cost primarily refers to

$$F^{B} = \sum_{b=1}^{N_B} I_{Cb}^{B} P_b^{B} \tag{11}$$

where I_{Cb}^{B} is the annualized investment cost per unit capacity.

The operating cost consists of the new energy loss cost and the operating cost of the regulating power sources, expressed as:

$$\begin{aligned} F^{Opr} &= \sum_{t=1}^{N_T}\sum_{k=1}^{N_K} I_R^B P_{k,t}^{R,Cur} + F^I \\ &= \sum_{t=1}^{N_T}\sum_{k=1}^{N_K} I_R^B P_{k,t}^{R,Cur} + \sum_{t=1}^{N_T}\sum_{i=1}^{N_I} I_g^P P_{i,t}^{I} \end{aligned} \tag{12}$$

where $\sum_{t=1}^{N_T}\sum_{k=1}^{N_K} I_R^B P_{k,t}^{R,Cur}$ represents the new energy loss cost; I_R^B is the wind/photovoltaic curtailment cost.

The second objective is to maximize the outbound electricity guarantee rate. Therefore, the optimal configuration model can balance economy and outbound power reliability, which can be expressed as:

$$obj\begin{cases} \min f_1(P_b^B) = \sum_{b=1}^{N_B} I_{Cb}^{B} P_b^{B} \\ + \sum_{t=1}^{N_T}\left(\sum_{k=1}^{N_K} I_R^B P_{k,t}^{R,Cur} + \sum_{i=1}^{N_I} I_g^P P_{i,t}^{I} \right) \\ \min f_2(P_b^B) = \dfrac{\sum_{t=1}^{T} L_t}{\sum_{t=1}^{T} L_t - \sum_{t=1}^{T} L_t^{lack}} \end{cases}$$

$$s.t.\begin{cases} P_{k,t}^{R} + P_{k,t}^{R,Cur} = \omega_{k,t}^{R} C_k^{R}, & \forall k,t \\ E_{b,t}^{B} - E_{b,t-1}^{B} = \eta_b^B P_{b,t}^{B,cha} - P_{b,t}^{B,dis} / \eta_b^B, & \forall b,t \\ E_{b,t=0}^{B} = E_{b,t=N_T}^{B} = \lambda_b^{B,min} H_b P_b^B, & \forall b,t \\ P_{k,t}^{R} + P_{i,t}^{I} + P_{b,t}^{B,dis} - P_{b,t}^{B,cha} - P_{L,t} = F_t, & \forall k,b,t \\ F_t + L_t^{lack} = L_t, & \forall t \\ P_{k,t}^{R}, P_{k,t}^{R,Cur} \ge 0, & \forall k,t \\ \alpha_{min} C_i^I \le P_{i,t}^{I} \le \alpha_{max} C_i^I, & \forall i,t \\ 0 \le P_{b,t}^{B,cha}, P_{b,t}^{B,dis} \le P_b^B, & \forall b,t \\ 0 \le E_{b,t}^{B} \le C_b^B, & \forall b,t \\ 0 \le L_t^{lack} \le L_t, & \forall t \end{cases} \tag{13}$$

By solving Equation (13), the energy storage configuration schemes under different scenarios can be optimally calculated.

The optimal configuration model of energy storage for the new energy base is a typical multi-objective and multi-constraint optimization problem.

3. Optimal Configuration and Fuzzy Decision-making of Energy Storage in a New Energy Base

3.1. Multi-objective Particle Swarm Optimization Algorithm

3.1.1. Basic Particle Swarm Optimization Algorithm

In the basic PSO algorithm, the velocity and position of each particle are updated:

$$\begin{aligned} V_{i,d}^{K+1} &= wV_{i,d}^{K} + c_1 r_1 \times (P_{i,d}^{K} - x_{i,d}^{K}) \\ &+ c_2 r_2 \times (G_{i,d}^{K} - x_{i,d}^{K}) \end{aligned} \tag{14}$$

$$x_{i,d}^{K+1} = x_{i,d}^{K} + V_{i,d}^{K+1} \tag{15}$$

where K is the number of iterations; $V_{i,d}^{K}$ is the velocity of particle i in the d-dimensional space; w is the inertia weight of the particle velocity; c_1 and c_2 are learning factors; r_1 and r_2 are random numbers distributed in $[0,1]$; $P_{i,d}^{K}$ represents the personal best of particle i; $G_{i,d}^{K}$ represents the global best solution in the particle swarm; and $x_{i,d}^{K}$ represents the position of particle i in the d-dimensional space.

3.1.2. Multi-objective Particle Swarm Optimization Algorithm

Based on the Pareto optimality principle, this paper improves the basic PSO algorithm to meet the requirements of solving the multi-objective optimization model in energy storage optimal configuration. The specific improvements include:

1) Particle position update. The inertia weight is set to decrease as the number of iterations increases. When the number of iterations is small, w is greater than c_1 and c_2 to enhance the diversity of solutions; as the number of iterations increases, w becomes smaller than c_1 and c_2 to enhance the convergence of solutions. The specific expression for w is:

$$w = \exp\left(\frac{1}{iter - MaxIt}\right) \tag{16}$$

where $iter$ is the current number of iterations, and $MaxIt$ is the maximum number of iterations.

2) Determination of particle dominance relationship. This paper uses a method based on the Pareto dominance relationship to determine the dominance relationship between two particles. Due to the presence of constraints, all obtained Pareto solutions are feasible solutions.

3) Update of non-inferior solutions. In the traditional PSO algorithm, when updating the optimal solution of a particle, if there is no dominance relationship between the new particle and the old particle, one of them will be randomly selected as the optimal particle and the other will be discarded, even though both particles could potentially be non-inferior solutions. However, due to the large number of constraints in the problem, this may lead to too few non-inferior solutions, thereby resulting in insufficient population diversity. For this reason, after selecting the optimal particle according to the traditional method, both solutions without a dominance relationship will serve as the basis for the subsequent update of the non-inferior solution set, so as to enhance the diversity of solutions.

3.2. Energy Storage Optimization of New Energy Base Based on MOPSO

After determining the operation simulation cycle and specifying the time-series outbound power demand, local time-series demand data, typical new energy time-series data, parameters of active regulating power sources, and basic technical parameters of energy storage within the simulation cycle, MOPSO can be utilized.

1. Data preparation. This mainly includes typical daily and monthly time-series data of wind and photovoltaic power; time-series data of outbound power delivery; typical daily and monthly time-series data of local load demand; parameters of active regulating power sources, and basic technical parameters of energy storage.

2. Setting algorithm parameters. This includes the maximum number of iterations, population size, and learning factor values.

3. Initialization. Randomly generate 300 sets of initial populations for P_b^B , $P_{k,t}^{R,cur}$, $P_{i,t}^{I}$, and L_t^{lack} within the constraint ranges.

4. Calculate the fitness values of the initial population using Equation (13) and assign the optimal position of the particle as its initial position.

5. Screening of the initial non-inferior solution set. The specific rule is: for particle i, as long as there exists a particle j that can dominate it, it is definitely not a non-inferior solution; conversely, if no particle j can dominate it, it is a non-inferior solution.

6. Enter the iterative loop, recalculate the inertia weight w according to Equation (17), and randomly select a particle from the non-inferior solutions as the global best of the population.

7. Calculate the fitness value of the new population using Equation (13).

8. Update the personal best of the particles. Select the dominating particle from the current new particle and the personal best particle according to the Pareto dominance principle. If neither particle dominates the other, randomly select one particle as the personal best.

9. Update the solution set. Use the update principle to obtain the updated set from the combined collection of the existing non-inferior solutions and the personal best particles.

10. Cyclically execute steps 5 to 8 and perform the termination condition check. If the condition is met, terminate the calculation.

3.3. Decision-Making of Optimal Configuration Scheme Based on Fuzzy Evaluation

The energy storage configuration schemes obtained by the algorithm steps in Section 2.2 form a Pareto optimal solution set. A suitable method is needed to provide engineers and technicians with the final energy storage configuration scheme. This paper adopts the fuzzy mathematics method to calculate the satisfaction degree of each scheme, and then determines the scheme with the maximum satisfaction degree as the final configuration scheme. The calculation expression for the fuzzy membership degree of satisfaction is as follows:

$$\xi_i^n = \begin{cases} 1, & F_i^n \le F^{n,\min} \\ \dfrac{F^{n,\max} - F_i^n}{F^{n,\max} - F^{n,\min}}, & F^{n,\min} < F_i^n < F^{n,\max} \\ 0, & F_i^n \ge F^{n,\max} \end{cases} \quad (17)$$

where F_i^n is the value of the n-th dimensional objective function for the i-th optimal solution; $F^{n,\min}$ and $F^{n,\max}$ are the minimum and maximum values of the n-th objective function in the obtained Pareto optimal solution set, respectively.

The degree for optimal solution is defined as:

$$\xi_i^* = \frac{\sum_{n=1}^{2} \xi_i^n}{\sum_{k=1}^{N_p} \sum_{n=1}^{2} \xi_k^n} \quad (18)$$

where N_p is the number of Pareto solutions. In this paper, the one with the maximum satisfaction value is selected as the best compromise configuration scheme. The overall algorithmic flow is shown in Figure 1.

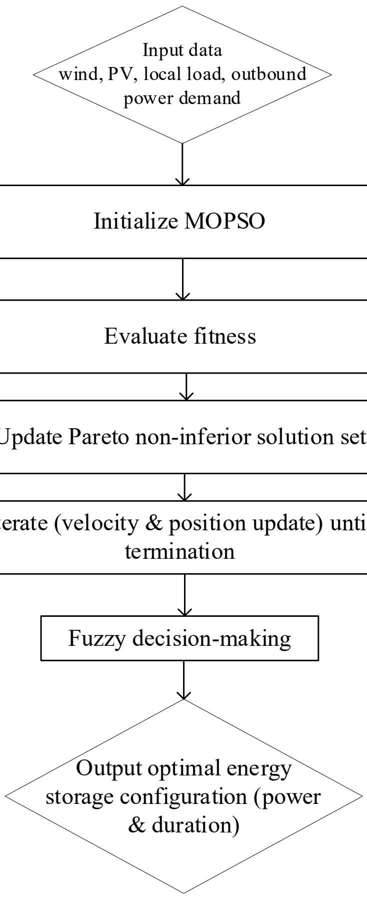

Figure 1. Algorithmic flow

4. Case Study Analysis

Taking a new energy base in northern China, the planned annual capacity of new energy is 20 million kW, including 16 million kW of wind power and 4 million kW of photovoltaic power. For the receiving-end system connected to the outbound delivery channel, a certain capacity of active regulating power sources is installed. These active regulating power sources possess a certain degree of monthly active power generation regulation capability. Within a day, the transmission mode is arranged based on the short-term power generation characteristics of new energy. Generally, a three-stage transmission mode is adopted intra-day, and the transmission mode varies slightly depending on the season, as shown in Figure 2.

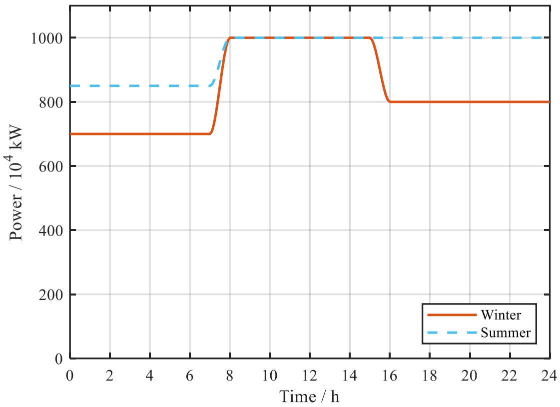

Figure 2. Daily power outbound delivery curve in winter and summer

The local power demand curve within the base and the typical output curves are required to conduct production simulation and optimally configure the required energy storage capacity. Figure 3 illustrates the typical daily operation simulation results, including the outbound power demand and local power demand curves, wind and photovoltaic power output curves, and active regulating power source output curves.

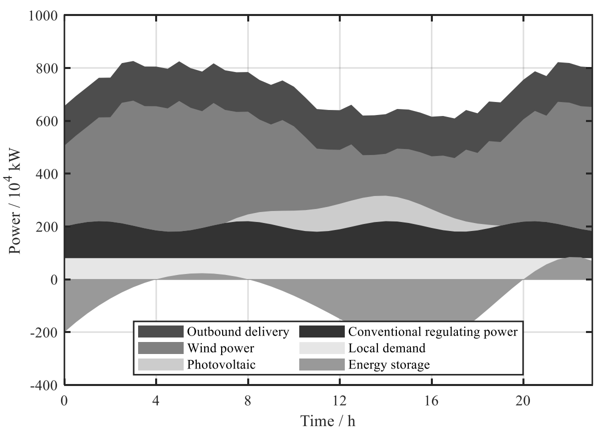

Figure 3. Typical daily operation simulation diagram

Figure 4 shows the new energy utilization and the charging and discharging conditions of the energy storage system during the typical day shown in Figure 3. Although there is still some new energy loss, the comprehensive operating cost is minimized.

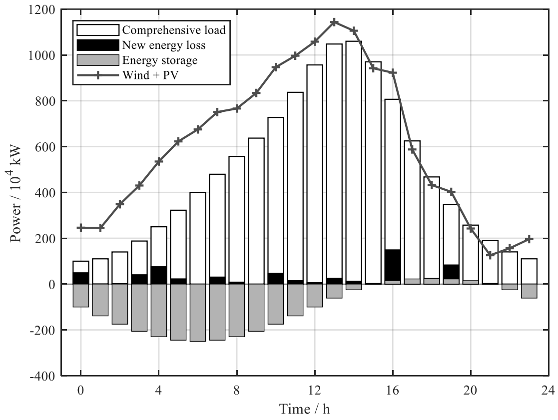

Figure 4. New energy utilization and charging and discharging conditions of the energy storage system

The results in Figures 3 and 4 indicate that charging and discharging can compensate for the active power output of new energy. This not only improves the utilization efficiency of new energy but also ensures the reliability of the outbound power delivery.

This paper focuses on the power and energy balance over a long time scale. A duration of 6 hours is typically selected. This paper first analyzes the energy storage capacity requirements under scenarios with energy storage durations of 4 hours, 6 hours, and 8 hours.

Under the 6-hour energy storage duration, the Pareto optimal frontier solutions are shown in Figure 4. The MOPSO-based energy storage configuration scheme proposed in this paper outperforms the calculation results of NSGAII in terms of both economy and reliability.

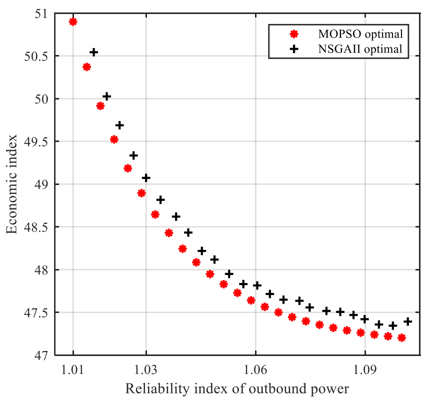

Figure 5. Pareto optimal frontier solution.

The required energy storage capacity decreases, while the new energy utilization efficiency and the outbound electricity guarantee rate improve. This is because the duration strengthens its support capability in continuous scenarios without wind or sunlight. However, since the increase in energy storage leads to a substantial rise in costs, the comprehensive power generation cost also significantly increases. The Pareto optimal frontier solution is shown in Figure 5.

To further analyze the variation trends of economic indicators as the energy storage duration increases, the technical and economic indicators are normalized (actual value / maximum value). Figure 6 indicates that the growth rates of new energy utilization efficiency and the outbound electricity guarantee rate slow down, but the growth rate of the comprehensive power generation cost increases significantly.

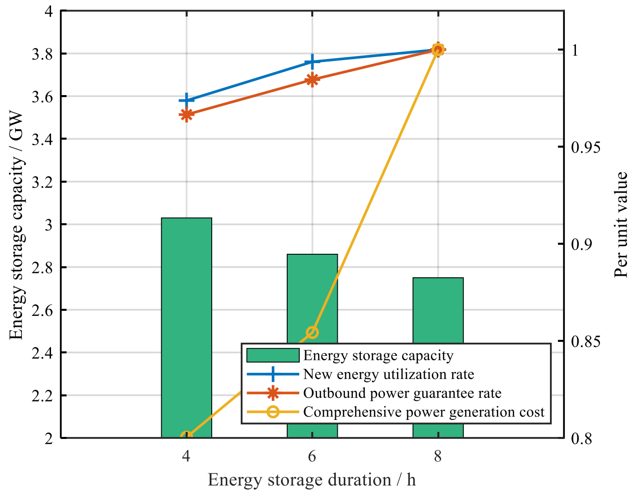

Figure 6. Trend of technical and economic indicators under different energy storage durations

With the deep implementation of the "Dual Carbon" goals, conventional power sources in the receiving-end systems are gradually being phased out, and the reliance on external power demands will gradually increase. The utilization hours of the power outbound delivery channels for new energy bases will also steadily rise. To ensure the outbound electricity guarantee rate, the demand for energy storage in new energy bases will also increase. Therefore, selecting the operating condition with a 6-hour energy storage duration, this paper analyzes the energy storage demands of the new energy base under 5 scenarios where the utilization hours of the outbound delivery channel are 4500 h, 4750 h, 5000 h, 5250 h, and 5500 h, respectively.

As the utilization hours of the outbound delivery channel increase, the outbound delivery power of the new energy base also increases accordingly, which in turn increases the energy storage demand. The new energy utilization rate continuously improves, but the outbound electricity guarantee rate decreases to some extent. The specific variation trends are shown in Figure 7.

With the increase in outbound delivery power, the investment in energy storage gradually rises, causing the comprehensive power generation cost to increase significantly from 0.300 2 CNY/(kW·h) to 0.406 1 CNY/(kW·h). With the development of energy storage technology, the investment cost of energy storage is expected to decrease, and the comprehensive power generation cost of the new energy base will also decrease accordingly.

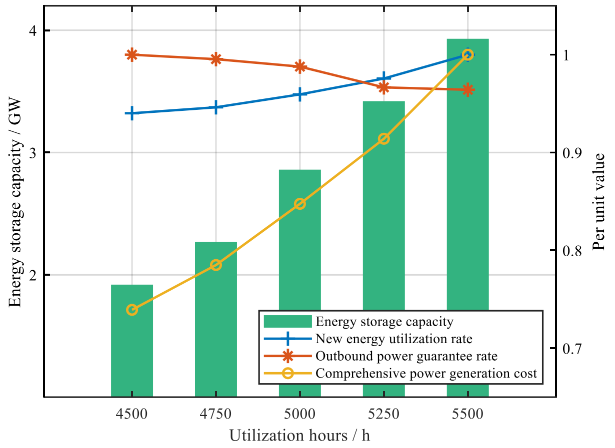

Figure 7. Variation trend of technical and economic indicators under different utilization hours of outbound delivery channels

In the future novel power system, energy storage serves as the primary regulating power source for new energy bases. It is the key to ensuring reliable outbound delivery of new energy while simultaneously accommodating internal demands, making its reasonable planning crucial [23-25]. From the above computational analysis, it is clear that energy storage demand is closely related to the outbound power demand. However, limited by current energy storage cost factors, as the energy storage capacity increases, the comprehensive power generation cost of the new energy base continues to rise.

To further validate the computational efficiency and search stability of the proposed modified MOPSO algorithm, the convergence characteristics are compared with the traditional NSGA-II algorithm, as shown in Figure 8. By utilizing the non-linear adaptive decreasing inertia weight, it ultimately yields a lower and more stable system operating cost. This proves the superiority of the proposed algorithmic framework in solving high-dimensional optimization problems.

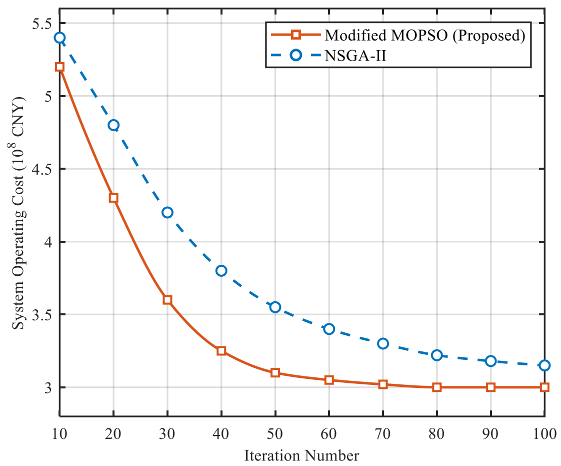

Figure 8. Comparison of convergence characteristics between the modified MOPSO and NSGA-II

Furthermore, after obtaining the Pareto optimal solution set, selecting the most appropriate configuration requires quantitative evaluation. Figure 9 illustrates the distribution of fuzzy satisfaction degrees across the non-dominated Pareto solutions. The fuzzy decision-making algorithm evaluates both the economic cost and the reliability indices simultaneously. The solution with the highest membership degree (marked with a red star) is dynamically identified as the best compromise configuration scheme. This data-driven evaluation process effectively resolves the multi-criteria decision-making bottleneck, providing a robust computational tool for grid planners.

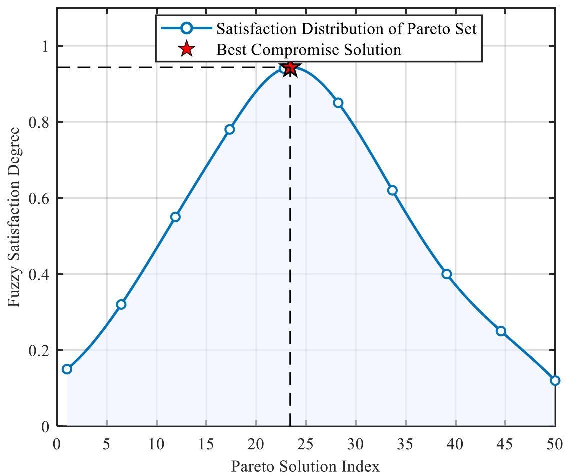

Figure 9. Fuzzy satisfaction degree distribution of the Pareto optimal solution set

5. Conclusion

In response to the issue of limited regulating power sources in new energy bases and the need for a reasonable energy storage configuration, this paper proposes an energy storage optimal configuration model for new energy bases that balances local demand and outbound delivery. Taking a planning scenario of a new energy base in northern China, the proposed method was calculated and analyzed.

1. Under given boundary conditions, such as outbound and local power demands, and typical active power outputs of new energy, the algorithm proposed in this paper can obtain the optimal energy storage configuration that balances the operational economy and the reliability of outbound delivery;

2. Fuzzy decision-making can provide a compromise energy storage configuration scheme, balancing the contradiction between economy and the reliability of outbound power delivery;

3. As the outbound power demand increases, the demand for energy storage capacity also increases. Under current technical and economic costs, the comprehensive power generation cost of the new energy base continues to rise.

Currently, energy storage is developing rapidly, and the technical and economic indicators of various energy storage technologies are constantly changing. When configuring energy storage for new energy bases, the changes in these technical and economic indicators, especially economic costs, should be fully considered, and the configuration results should be revised in a timely manner.

Acknowledgements

This work was supported by the Science and Technology Project of the State Grid Corporation of China (Project No. 522830250005).

References

[1] S. F. Santos, M. Gough, D. Z. Fitiwi, A. F. Silva, M. Shafie-Khah, and J. P. Catalão, “Influence of battery energy storage systems on transmission grid operation with a significant share of variable renewable energy sources,” IEEE Systems Journal, vol. 16, no. 1, pp. 1508–1519, Mar. 2021.

[2] T. Conlon, M. Waite, and V. Modi, “Assessing new transmission and energy storage in achieving increasing renewable generation targets in a regional grid,” Applied Energy, vol. 250, pp. 1085–1098, Sep. 2019.

[3] M. Peker, A. S. Kocaman, and B. Y. Kara, “Benefits of transmission switching and energy storage in power systems with high renewable energy penetration,” Applied Energy, vol. 228, pp. 1182–1197, Oct. 2018.

[4] R. Golombek, A. Lind, H. K. Ringkjøb, and P. Seljom, “The role of transmission and energy storage in European decarbonization towards 2050,” Energy, vol. 239, p. 122159, Jan. 2022.

[5] J. Liu, H. Hu, S. S. Yu, and H. Trinh, “Virtual power plant with renewable energy sources and energy storage systems for sustainable power grid-formation, control techniques and demand response,” Energies, vol. 16, no. 9, p. 3705, Apr. 2023.

[6] Y. Wu, J. Fang, X. Ai, X. Xue, S. Cui, X. Chen, and J. Wen, “Robust co-planning of AC/DC transmission network and energy storage considering uncertainty of renewable energy,” Applied Energy, vol. 339, p. 120933, Jun. 2023.

[7] O. B. Adewumi, G. Fotis, V. Vita, D. Nankoo, and L. Ekonomou, “The impact of distributed energy storage on distribution and transmission networks’ power quality,” Applied Sciences, vol. 12, no. 13, p. 6466, Jun. 2022.

[8] M. Vellingiri, M. Rawa, S. Alghamdi, A. A. Alhussainy, Z. M. Ali, R. A. Turky, and S. H. A. Aleem, “Maximum hosting capacity estimation for renewables in power grids considering energy storage and transmission lines expansion using hybrid sine cosine artificial rabbits algorithm,” Ain Shams Engineering Journal, vol. 14, no. 5, p. 102092, May 2023.

[9] J. Li, Z. Zhao, D. Xu, P. Li, Y. Liu, M. A. Mahmud, and D. Chen, “The potential assessment of pump hydro energy storage to reduce renewable curtailment and CO_2 emissions in Northwest China,” Renewable Energy, vol. 212, pp. 82–96, Aug. 2023.

[10] M. Arun, S. Samal, D. Barik, S. S. Chandran, K. Tudu, and S. Praveenkumar, “Integration of energy storage systems and grid modernization for reliable urban power management toward future energy sustainability,” Journal of Energy Storage, vol. 114, p. 115830, Mar. 2025.

[11] J. M. Kluger, M. N. Haji, and A. H. Slocum, “The power balancing benefits of wave energy converters in offshore wind-wave farms with energy storage,” Applied Energy, vol. 331, p. 120389, Feb. 2023.

[12] K. Shafiei, S. G. Zadeh, and M. T. Hagh, “Planning for a network system with renewable resources and battery energy storage, focused on enhancing resilience,” Journal of Energy Storage, 2024, 87: 111339.

[13] L. Malka, A. Daci, A. Kuriqi, P. Bartocci, and E. Rrapaj, “Energy storage benefits assessment using multiple-choice criteria: the case of Drini River Cascade, Albania,” Energies, vol. 15, no. 11, p. 4032, May 2022.

[14] S. Liu, J. Yan, Y. Yan, H. Zhang, J. Zhang, Y. Liu, and S. Han, “Joint operation of mobile battery, power system, and transportation system for improving the renewable energy penetration rate,” Applied Energy, vol. 357, p. 122455, Mar. 2024.

[15] Y. Ding, X. Chen, and J. Wang, “Deep reinforcement learning-based method for joint optimization of mobile energy storage systems and power grid with high renewable energy sources,” Batteries, vol. 9, no. 4, p. 219, Apr. 2023.

[16] M. Akmal, O. Umeh, A. Yusuf, and A. Onyenagubom, “Impact of distributed generation and battery energy storage systems on an interconnected power system,” in Proc. 2024 7th Int. Conf. Energy Conservation Efficiency (ICECE), Mar. 2024, pp. 1–6.

[17] X. Deng, T. Lv, J. Xu, X. Hou, and F. Liu, “Assessing the integration effect of inter-regional transmission on variable power generation under renewable energy consumption policy in China,” Energy Policy, vol. 170, p. 113219, Nov. 2022.

[18] J. Liu, Z. Huang, M. Fan, J. Yang, J. Xiao, and Y. Wang, “Future energy infrastructure, energy platform and energy storage,” Nano Energy, vol. 104, p. 107915, Dec. 2022.

[19] S. Ma, Z. Meng, Y. Wu, and D. Xin, “A bi-objective optimization framework for configuration of battery energy

storage system considering energy loss and economy," Energy Exploration & Exploitation, vol. 43, no. 2, 564-586, 2025.

[20] M. Staadecker, J. Szinai, P. A. Sánchez-Pérez, S. Kurtz, and P. Hidalgo-Gonzalez, "The value of long-duration energy storage under various grid conditions in a zero-emissions future," Nature Communications, vol. 15, no. 1, p. 9501, Nov. 2024.

[21] L. Li, B. Wang, K. Jiao, M. Ni, Q. Du, Y. Liu, and C. Wang, "Comparative techno-economic analysis of large-scale renewable energy storage technologies," Energy and AI, vol. 14, p. 100282, Nov. 2023.

[22] Mena, R., D. R. Godoy, F. Kristjanpoller, and P. Viveros, "A multi-objective two-stage stochastic unit commitment model for wind and battery-integrated power systems," Journal of Energy Storage, vol. 89, p. 111723, Jun. 2024.

[23] C. Chen, J. Wang, Z. Yu, Y. Ma, Y. Wang, L. Fan, R. Ding, and H. Li, "Review and Outlook of Autonomous Unit Planning of Distribution Network," Electric Power, vol. 56, no. 12, pp. 9–19, Dec. 2023. (In Chinese)

[24] X. Zhu, G. Ruan, H. Geng, H. Liu, M. Bai, and C. Peng, "Multi-objective sizing optimization method of microgrid considering cost and carbon emissions," IEEE Transactions on Industry Applications, 2024, 60(4), 5565-5576.

[25] M. Y. Worku, "Recent Advances in Energy Storage Systems for Renewable Source Grid Integration: A Comprehensive Review," Sustainability, vol. 14, no. 10, pp. 5985, 2022.